

Chaotic Mixing in a Twisted Pipe: Optimisation of Heat, Mass Transfer and RTD

B.T. Kuan¹, D.R. Lester¹, W. Yang¹ and G. Metcalfe²

¹Mineral Resources Flagship
 Commonwealth Scientific and Industrial Research Organisation, Clayton 3168, Australia

²Manufacturing Flagship
 Commonwealth Scientific and Industrial Research Organisation, Highett 3190, Australia

Abstract

It is now well-known that chaotic advection in laminar flow significantly impacts scalar transport – heat, mass and residence time distribution (RTD). In context of twisted pipes, such phenomena are relevant to a wide range of applications which demand rapid heat and mass transport ranging from micro-fluidics and continuous chemical processing to bioreactors. A general theoretical framework linking the three modes of transport was described and applied to optimise the performance of a twisted pipe in terms of mixing, heat transfer and ability to produce a narrow RTD. The work indicates that it is possible to optimise all three aspects of the twisted pipe in a single analysis.

Introduction

Chaotic advection in laminar flow provides a transport mechanism for scalars such as heat and mass with similar characteristics to that of turbulent flow [3, 5]. Mass and heat transfer may be readily accelerated, whilst RTD variance is suppressed, all of which are highly beneficial for a wide range of engineering applications in the laminar flow regime. In flow chemistry, for example, accelerated heat and mass transport respectively are critical for improving mixing and achieving better control of process temperature, whilst product uniformity is directly related to narrowness of the RTD. As many engineering processes require all three modes to be simultaneously optimised, there exists a direct need to understand how this might be achieved in chaotic flows.

There exists a deep connection between the three transport modes (heat, mass, RTD) which points to a new methodology for simultaneous optimisation. In this study, we use the twisted pipe flow [3, 12, 25] as a prototypical example to both demonstrate the underlying concepts and perform an optimisation process. We consider how the eigenmode structure in a twisted pipe controls both transverse and axial scalar dispersion, leading to a framework under which global optimisation is possible.

Background

The twisted pipe flow comprises of a series of pipe bends connected in series with an angular offset (i.e. twist) between two consecutive bends (Figure 1). At certain Reynolds number, fluid passing through any bend induces a secondary flow that arises as the faster fluid stream near the pipe axis moves towards the concave side of the bend [6], resulting in the well-known formation of counter rotating vortices [7, 8] known classically as Dean roll cells. This produces periodic re-orientation of the flow which is critical for sustaining chaotic advection in the pipe.

Jones et al. [12] found that the twist angle has considerable effect on transverse scalar transport, specifically that such particular twist angles can generate chaotic mixing within the twisted pipe flow. The twisted pipe flow falls into a wide class of periodically reoriented duct flows, e.g. RAM [15], SMW mixer [23], etc,

which has received widespread attention. Various other studies have looked into different twisted pipe configurations to optimise chaotic mixing and heat transfer, for example [1, 18, 19, 25]. At certain twist angles, reorientation of the secondary flow repetitively stretches and folds the trajectories of fluid particles, producing exponential separation of neighbouring fluid particles and highly striated material distributions. This process is the hallmark of chaotic advection, and leads to highly efficient mixing.

In conjunction with chaotic advection, thermal or molecular diffusion transport acts to impart significantly accelerated irreversible dispersion, leading to rapid heat and mass transfer. It is known that enhanced transverse dispersion and hence mixing suppresses axial dispersion [13], leading to a narrower RTD [3, 21]. This suggests a deep connection between chaotic mixing and RTD as demonstrated indirectly by Mezić et al. [17] who related RTD to Poincaré map in pipes.

Theory

Twisted pipe flow is described as a periodically reoriented duct flow with axial coordinate z which aligns with the direction of the bulk flow, and transverse coordinates (r, θ) . The 3D periodic velocity field $\mathbf{u}(\mathbf{x})$ can be written as

$$\mathbf{u}(r, \theta, z + L) = R_\theta[\mathbf{u}(r, \theta, z)] \quad (1)$$

where R_θ is a rotation operator about the z -axes, and $\mathbf{x} = r, \theta, z$ forms an orthogonal coordinate system. Transport of scalars such as heat and mass in this flow can be described by the dimensionless steady advection-diffusion equation (ADE) for the scalar quantity ϕ representing heat or mass concentration

$$\nabla \cdot (\mathbf{u}\phi) = \frac{1}{Pe} \nabla^2 \phi + S(\mathbf{x}) \quad (2)$$

where Pe is Peclet number for heat scalar ADE, and is replaced with Schmidt number (Sc) for mass scalar AED; S is a domain source. The ADE (2) is subject to the initial condition $\phi(r, \theta, 0) = \phi_0$, and either Dirichlet or Neumann boundary conditions respectively at the pipe wall:

$$\phi|_{r=R} = f_1(\mathbf{x}) \quad (3)$$

$$\left. \frac{\partial \phi}{\partial r} \right|_{r=R} = f_2(\mathbf{x}) \quad (4)$$

The Dirichlet boundary condition (3) corresponds to problems with a fixed value at wall, e.g. wall heating. The Neumann boundary condition (4) represents zero flux condition at the wall, e.g. mass transport and RTD evolution. The probability density function (PDF) P of the residence time is given by an unsteady ADE [24]

$$\nabla \cdot (\mathbf{u}P) = \frac{1}{Pe} \nabla^2 P - \frac{\partial P}{\partial s} \quad (5)$$

with s being age of the fluid particles. This is remarkably similar to equation (2). It demonstrates a close connection between axial/transverse dispersion and RTD similar to that exists for Taylor-Aris dispersion.

Based on Liu and Haller [16], Lester et al. [14] established that, for a spatially periodic flow where $\mathbf{u}(z) = \mathbf{u}(z + L)$, the solution to the ADE with $S(\mathbf{x}) = f_1(\mathbf{x}) = f_2(\mathbf{x}) = 0$ is the sum of a finite number of strange eigenmodes (so-called as the eigenmodes have non-trivial structure in the limit $Pe \rightarrow \infty$)

$$\phi(r, \theta, z) = \langle \phi_0 \rangle + \sum_{k=0}^K \alpha_k e^{-\lambda_k z} \psi_k(r, \theta, z) + O(e^{-pz}) \quad (6)$$

where $\langle \rangle$ denotes averaging over cross-section; α_k weighting functions to be determined from the initial conditions ϕ_0 ; λ_k the (possibly complex) decay rate; $\psi_k(r, \theta, z)$ the k th strange eigenmode; O an arbitrary small fast decaying term. With reference to [15] who have solved ADE (2) based on similar boundary conditions used (i.e. condition (3) or (4)). They are, however, insensitive to values of S , f_1 and $f_2 \neq 0$. Also, non-zero S and arbitrary values of f_1 and f_2 all produce asymptotic transport that is governed by λ_0 .

Splitting ϕ into a fully-developed part $\bar{\phi}$ and a zero-mean part $\tilde{\phi}$ and ignoring the O term leads to

$$\tilde{\phi}(r, \theta, z) = \sum_{k=0}^K \alpha_k e^{-\lambda_k z} \psi_k(r, \theta, z) \quad (7)$$

With eigenmodes ordered such that $|\lambda_k| < |\lambda_{k+1}|$. For a pipe of finite length, equation (6) thus suggests that the slowest decaying eigenmode corresponding to $k=0$ dominates as z increases and can be approximated as

$$\lim_{z \rightarrow \infty} \tilde{\phi}(r, \theta, z) \rightarrow \alpha_0 e^{-\lambda_0 z} \psi_0(r, \theta, z) \quad (8)$$

where ψ_0 is the dominant eigenmode and λ_0 the associated decay rate. Hence, λ_0 solely controls asymptotic transport of scalars and can be used to optimise heat and mass transfer in processes based on chaotic advection. We demonstrate this approach in this paper.

Problem Description

Strange eigenmode decomposition suggests that in an axially periodic flow such as that in a twisted pipe, a passive scalar (e.g. mass or heat) transport is asymptotically governed by λ_0 , generating a convenient basis for optimization. For mass transport and heat transfer cases based on Neumann boundaries, the eigenmodes for both processes are the same. Hence, optimisation can be performed simultaneously. This approach, however, is not applicable to mass and heat transport under Dirichlet boundary conditions. Optimisation will then need to consider eigenmodes for mass and heat transport separately.

To verify this, we set out to numerically solve fluid motion and scalar transport in a twisted pipe to simulate the following scenarios:

1. Internal mixing with homogeneous Neumann boundary condition (4) and $f_2=0$;
2. Constant temperature wall heating with Dirichlet boundary condition (3) $f_1=1$;
3. RTD with homogeneous Neumann boundary condition $f_2=0$, and $S=1$.

To monitor the evolution of passive scalar variance and calculate its decay rate, a mixing index $\zeta(\phi)$ is defined as

$$\zeta(\phi) = \frac{\int_{\Omega} (\phi_i(x) - \langle \phi \rangle)^2 dx}{\int_{\Omega} (\langle \phi \rangle)^2 dx} \quad (9)$$

where ϕ denotes a scalar. For the internal mixing case, ζ is one at the inlet and approaches zero as $z \rightarrow \infty$. Thus, ζ quantifies homogeneity of ϕ at a given cross-section of the twisted pipe. The same applies to the wall heating and RTD cases, however, ζ can become infinitely large at the inlet where $\langle \phi \rangle = 0$.

The twisted pipe considered in this work consists of 24 identical 90° bend elements connected in series, each having a radius a of 15 mm and a turning radius R of 60 mm, yield bend ratio $a/R = 1/4$ (Figure 1). In forming a twisted pipe, the symmetry plane of each bend element is rotated by a constant twist angle φ away from its upstream counterpart along the z -axis. By adjusting φ , the twisted pipe can be configured into a coiled shape for $\varphi = 0^\circ$ (Figure 1b) and eventually turning into an undulating pipe for $\varphi = 180^\circ$ (Figure 1c).

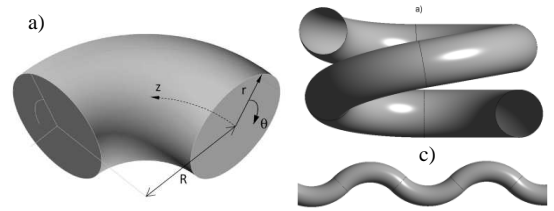


Figure 1. Twisted pipe geometry. a) coordinate system (r, θ, z) of a single bend element; b) coil configuration; c) undulating pipe configuration.

CFD simulations focused on the laminar flow regime with Dean number ranging from 100 to 1000, corresponding to a range $De > 106$ where four-vortex Dean rolls were observed in curved square duct [11]. For each value of Dean number De , we considered twist angles between 10° and 180° , where

$$De = Re \sqrt{a/R} \quad (10)$$

We are limiting our attention to $Pe = 10^5$ condition for all three scenarios where diffusion of the solute in the solvent is slow compared to convection, and hence chaos play a strong role in mixing.

Numerical Method

Fluid Mechanics

Flow of an incompressible Newtonian fluid passing through a twisted pipe under laminar condition at steady-state was solved using CFD. Mixing as represented by the diffusive transport of a passive scalar ϕ is also solved. The present work considers three scalars: normalised dye concentration C , normalised temperature T and residence time RT. The first two quantities range between 0 and 1.

Initial and Boundary Conditions

Fully-developed laminar flow properties are obtained from a separate straight pipe simulation and specified at the inlet of the twisted pipe.

For $\phi = T$ or RT, $\phi(r, \theta, 0) = 0$ was applied at the inlet. For the internal mixing case (i.e. $\phi = C$), the solute ($C = 1$) was initially separated from the solvent ($C = 0$) at the inlet as described by

$$\phi(r, \theta, 0) = \begin{cases} 1, & \theta \leq \pi \\ 0, & \theta > \pi \end{cases} \quad (11)$$

At the wall, no-slip condition was prescribed for the flow field. Neumann condition was applied for scalars C and RT. For scalar T , Dirichlet condition was used, i.e.

$$\phi(R, \theta, z) = 1 \quad (12)$$

Numerical Accuracy and Post Process

A uniform hexahedral mesh with 0.2 mm cells was constructed for the twisted pipe. This is expected to produce less than 3% error in the solution as suggested by a grid sensitivity study.

It was necessary to apply a residual value of 10^{-8} to all equations as required by [10].

The DMD algorithm of Schmid [22] was used to extract the dominant eigenmodes $\psi_k(r, \theta, z)$ and the corresponding eigenvalues λ_k from scalar distributions predicted by CFD.

Results and Discussions

Results of the twisted pipe simulations are compared to that of a straight pipe which represents a simplified tubular reactor which is widely used in flow chemistry. Note that length of the straight pipe is equivalent to the combined arc lengths of individual bends.

Internal Mixing

Mixing indices as defined in equation (8) were calculated for concentration scalar C at outlet planes of each bend elements, as shown for $De = 1000$ in Figure 2. The result indicates an exponential decay of $\zeta(C)$ over a large portion of the pipe length, suggesting that the local variance of C is falling asymptotically towards zero and therefore only dominant mode is present. $Re(\lambda_0)$ determined from the slopes of the curves in Figure 2 are the highest for twist angle 180° , i.e. $\varphi = 180^\circ$ case. It is -5.4 m^{-1} . λ_0 increases with twist angle, particularly when $\varphi > 90^\circ$. This is due to flow reversion which arises from periodic re-orientation of the bend. At $\varphi = 180^\circ$, Dean roll cells produced by a previous bend are forced to reverse directions in the following bend, causing significant folding and stretching of the filaments and thus strong mixing. For a straight pipe, the mixing index also decays asymptotically but more than 400 times slower.

Cross-sectional distributions of C for the $\varphi = 180^\circ$ case under the same condition are shown in Figure 3. Within the first four bends, the roll cells are clearly visible. Note that the mixing patterns between Bend 5 and 9 appear to switch periodically with Bends 5 and 7, and Bends 6 and 8 showing strong resemblance. This suggests a complex λ_0 .

DMD results are shown in Figure 4. It confirmed sub-harmonic or quasi-periodic nature of the dominant eigenmode which has a complex λ_0 of $(-5.82, 24.71) \text{ m}^{-1}$. Its real part is in good agreement with that determined from Figure 2 (i.e. -5.4 m^{-1}).

Wall Heating

Compared to internal mixing, transport of heat with a Dirichlet boundary is much slower due to weak time-dependence in the thermal boundary layer [9]. However, it did show a log-linear relation with z for the De and φ ranges tested (Figure 5). For the $De = 1000$, $\varphi = 160^\circ$ case which produced the strongest decay, $Re(\lambda_0)$ is -0.0585 m^{-1} compared to -0.00715 m^{-1} for the straight pipe. This is an improvement by a factor of more than 8.

Predicted transverse transport of heat scalar T is shown in Figure 6. The process is initiated by a local thickening of the thermal boundary layer near where the counter-rotating wall streams impinge onto each other and create a stagnant region at the wall. This is a direct consequence of a constant temperature boundary (Dirichlet condition) which acts to continually increase non-uniformity in the distribution of heat scalar. Unlike the case with a Neumann boundary, the DMD analysis here produced a positive λ_0 of $(0.103, 0) \text{ m}^{-1}$, suggesting a growth of the dominant eigenmode. It also gave a λ_1 of $(-0.51153, 0) \text{ m}^{-1}$ whose real part is significantly larger than -0.0585 m^{-1} . It is thus possible that the flow in the considered twisted pipe is still developing towards the

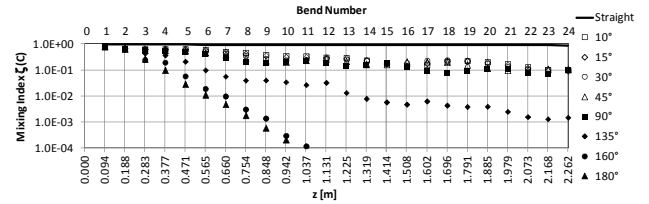


Figure 2. Predicted spatial evolution of mixing index of concentration scalar C for straight and undulating pipes at $De = 1000$.

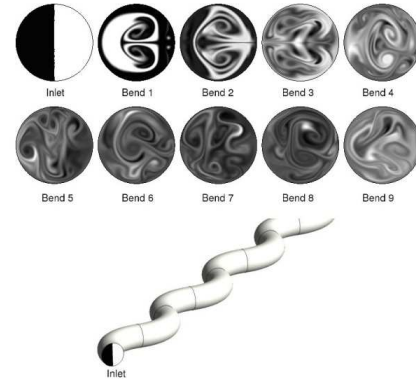


Figure 3. Top: Predicted cross-sectional distributions of C for the first 9 bends in the undulating pipe ($De = 1000$, $\varphi = 180^\circ$); Bottom: Geometric configuration of the bend elements with respect to the inlet.

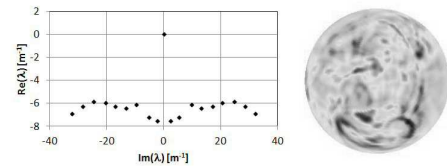


Figure 4. Left: DMD spectrum for the $De = 1000$, $\varphi = 180^\circ$ case; Right: dominant eigenmode corresponding to eigenvalue $(-5.82, 24.71) \text{ m}^{-1}$.

dominant eigenmode. This points to a need for extending the twisted pipe in the simulation. It is interesting to note a consistent pattern emerges in Bends 9 to 17 in Figure 6, and this is agrees with the λ_1 eigenmode as produced by the DMD.

Not all De and φ combinations tested produced positive λ_0 . The $De = 100$, $\varphi = 15^\circ$ case, for example, gave a λ_0 of $(-0.03125, 0) \text{ m}^{-1}$.

Residence Time

Residence times predicted by the end of the twisted pipes are compared for selected De in Figure 7. Note both E and RT quantities were normalised by mean residence time for a straight pipe under the same conditions. The theoretical curve refers to the classical result of a RT^{-3} tail for an ideal laminar straight tube flow [20]. For the straight pipe, discrepancies from the classical solution were due to the presence of a weak diffusion transport in the flow field.

It is evident that the RTD range is much narrower in twisted pipes compared to a straight pipe, and this tendency grows with increasing twist angle. With reference to Figure 2, this is directly associated with stronger transverse dispersion which produced rapid decay of $\zeta(C)$ and suppressed axial dispersion at large twist angles. The numerical results thus support the notion that the transverse mixing eigenmodes govern RTD evolution, and both processes can be optimised simultaneously with the dominant eigenvalue λ_0 for internal mixing. According to Figure 7, the twisted pipe sharpened the RTD by at least 40% compared to a straight pipe. At $De = 1000$, up to 70% of RTD sharpening is attainable with a large twist angle.

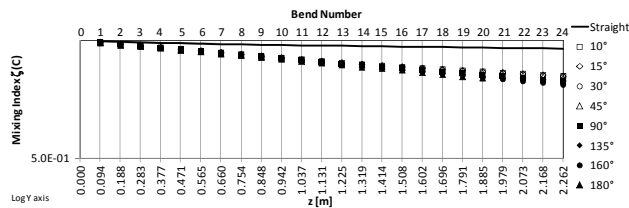


Figure 5. Predicted spatial evolution of mixing index of T for straight and undulating pipes at $De = 1000$.

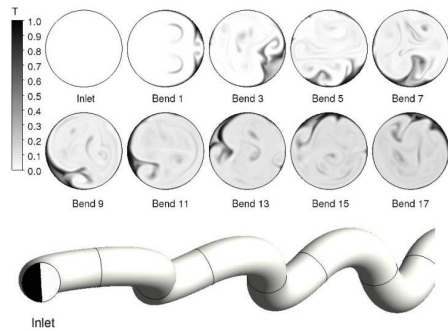


Figure 6. Top: Predicted cross-sectional distributions of T for selective bends in the twisted pipe ($De = 1000$, $\phi = 160^\circ$); Bottom: Geometric configuration of the bend elements with respect to the inlet.

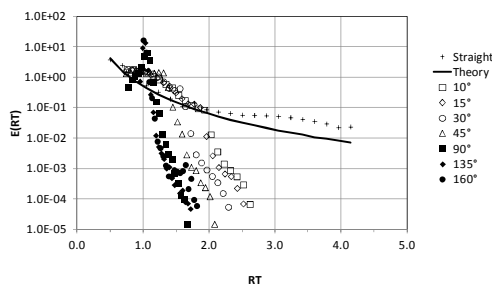


Figure 7. Predicted residence time distributions by the end of the twisted pipes ($De = 1000$).

Conclusions

Results from the present analysis support the theory [15] and illustrate the applicability of the dominant eigen value in optimising a laminar flow device. Using a twisted pipe as an example, we have demonstrated the connection between the dominant eigenmode for mixing and RTD evolution. Hence one can optimise the eigenmodes for mixing and expect to achieve the optimal RTD at the same time.

For pipes subject to a constant temperature, i.e. with Dirichlet boundary, no-slip condition at the wall dominates the transport of heat scalar. Hence, the process is controlled by a separate set of dominant eigenmodes. Pipes subject to a constant heat flux, i.e. with Neumann boundary, were not investigated. However, according to Lester et al. [15] and our result for RTD which is based on the same boundary condition, the heat transport process should also follow the mixing eigenmodes and hence can be optimised simultaneously.

The findings above provide basis for simultaneously optimising mass transport, heat transfer and RTD for a laminar flow device. This points to new possibilities in the design of a new generation of more efficient flow devices.

Acknowledgments

The authors acknowledge the financial support provided by Intelligent Processing Transformational Capability Platform (IPTCP).

References

- [1] Acharya, N., Sen, M., & Chang, H.-C., Heat Transfer Enhancement in Coiled Tubes by Chaotic Mixing, *Int. J. Heat Mass Trans.*, **35**(10), 1992, 2475-2489.
- [2] Berger, S.A., Talbot, L., & Yao, L.-S., Flow in Curved Pipes, *Ann. Rev. Fluid Mech.*, 1983, **15**, 461-512.
- [3] Castelain, C., Mokrani, A., Legentilhomme, P., & Peerhossaini, H., Residence Time Distribution in Twisted Pipe Flows: Helically Coiled System and Chaotic System, *Exp. Fluids*, **22**, 1997, 359-368.
- [4] Castelain, C., Berger, D., Legentilhomme, P., Mokrani, A., & Peerhossaini, H., Experimental and Numerical Characterisation of Mixing in a Steady Spatially Chaotic Flow by Means of Residence Time Distribution Measurements, *Int. J. Heat Mass Trans.*, **43**(19), 2000, 3687-3700.
- [5] Chaiken, J., Chevray, M., Tabor, & Tan Q.M., Experimental Study of Lagrangian Turbulence in a Stokes Flow, *Proc. R. Soc. Lond. A*, **408**, 1986, 165.
- [6] Dean, W.R., Note on the Motion of Fluid in a Curved Pipe, *Phil. Mag.*, **4**(20), 1927, 208-222.
- [7] Dean, W.R., The Stream-line Motion of Fluid in a Curved Pipe, *Phil. Mag.*, **5**(30), 1928, 673-685.
- [8] Eustice, J., Experiments of Streamline Motion in Curved Pipes, *Proc. Roy. Soc. London, Series A*, **85**, 1911, 119-131.
- [9] Ghosh, S., Leonard, A., & Wiggins, S., Diffusion of a Passive Scalar from a No-Slip Boundary into a Two-Dimensional Chaotic Advection Field, *J. Fluid Mech.*, **372**, 1998, 119-163.
- [10] Habchi, C., Harion, J.-L., Russeil, S., Bougeard, D., Hachem, F., & Elmarakbi, A., Chaotic Mixing by Longitudinal Vorticity, *Chem. Eng. Sci.*, **104**, 2013, 439-450.
- [11] Hille, P., Vehrenkamp, R., & Schulz-Dubois, E.O., The Development and Structure of Primary and Secondary Flow in a Curved Square Duct, *J. Fluid Mech.*, **151**, 1985, 219-241.
- [12] Jones, S.W., Thomas, O.M., & Aref, H., Chaotic Advection by Laminar Flow in a Twisted Pipe, *J. Fluid Mech.*, **209**, 1989, 335-357.
- [13] Jones, S.W., & Young, W.R., Shear Dispersion and Anomalous Diffusion by Chaotic Advection, *J. Fluid Mech.*, **280**, 1994, 149-172.
- [14] Lester, D.R., Rudman, M., Metcalfe, G., & Blackburn, H.M., Global Parametric Solutions of Scalar Transport, *J. Comp. Phys.*, **227**, 2008, 2032-3057.
- [15] Lester, D.R., Rudman, M., & Metcalfe, G., Low Reynolds Number Scalar Transport Enhancement in Viscous and Non-Newtonian Fluids, *Int. J. Heat Mass Trans.*, **52**, 2009, 655-664.
- [16] Liu, W., & Haller, G., Strange Eigenmodes and Decay of Variance in the Mixing of Diffusive Tracers, *Physica D*, **188**, 2004, 1-39.
- [17] Mezić, I., Wiggins, S., & Betz, D., Residence-Time Distributions for Chaotic Flows in Pipes, *CHAOS*, **9**(1), 1999, 173-182.
- [18] Mokrani, A., Castelain, C., & Peerhossaini, H., The Effects of Chaotic Advection on Heat Transfer, *Int. J. Heat Mass Trans.*, **40**(13), 1997, 3089-3104.
- [19] Peerhossaini, H., Castelain, C., & Le Guer, Y., Heat Exchanger Design Based on Chaotic Design, *Exp. Therm. Fluid Sci.*, **7**, 1993, 333-344.
- [20] Ruthven, D.M., The Residence Time Distribution for Ideal Laminar Flow in a Helical Tube, *Chem. Eng. Sci.*, **26**, 1971, 1113-1121.
- [21] Saxena, A.K., & Nigam, K.D.P., Coiled Configuration for Flow Inversion and Its Effect on Residence Time Distribution, *AIChE J.*, **30**(3), 1984, 363-368.
- [22] Schmid, P.J., Dynamic Mode Decomposition of Numerical and Experimental Data, *J. Fluid Mech.*, **656**, 2010, 5-28.
- [23] Singh, M.K., Anderson, P.D., & Meijer, H.E.H., Understanding and Optimizing the SMX Static Mixer, *Macromol. Rapid Commun.*, **30**, 2009, 362-376.
- [24] Vikhansky, A., Effect of Diffusion on Residence Time Distribution in Chaotic Channel Flow, *Chem. Eng. Sci.*, **63**, 2008, 1866-1870.
- [25] Yamagishi, A., Inaba, T., & Yamaguchi, Y., Chaotic Analysis of Mixing Enhancement in Steady Laminar Flows Through Multiple Pipe Bends, *Int. J. Heat Mass Trans.*, **50**, 2007, 1238-1247.